Dissecting Arabidopsis Gβ Signal Transduction on the Protein Surface[1][W][OA]

Kun Jiang, Arwen Frick-Cheng, Yuri Trusov, Magdalena Delgado-Cerezo, David M. Rosenthal, Justine Lorek, Ralph Panstruga, Fitzgerald L. Booker, José Ramón Botella, Antonio Molina, Donald R. Ort, and Alan M. Jones*

Departments of Biology (K.J., A.F.-C., A.M.J.) and Pharmacology (A.M.J.), University of North Carolina, Chapel Hill, North Carolina 27599–3280; School of Agriculture and Food Science, University of Queensland, Brisbane, Queensland 4072, Australia (Y.T., J.R.B.); Centro de Biotecnología y Genomica de Plantas, Universidad Politécnica de Madrid, Campus de Montegancedo, E–28223 Pozuelo de Alarcon, Madrid, Spain (M.D.-C., A.M.); Global Change and Photosynthesis Research Unit, Agricultural Research Unit, United States Department of Agriculture, Institute for Genomic Biology, Urbana, Illinois 61801 (D.R., D.R.O.); RWTH Aachen University, Institute for Biology I, Unit of Plant Molecular Cell Biology, D–52056 Aachen, Germany (J.L., R.P.); United States Department of Agriculture, Plant Science Research Unit, Raleigh, North Carolina 27607 (F.L.B.); and Department of Plant Biology and Crop Sciences, University of Illinois, Urbana, Illinois 61801 (D.R.O.)

The heterotrimeric G-protein complex provides signal amplification and target specificity. The Arabidopsis (*Arabidopsis thaliana*) Gβ-subunit of this complex (AGB1) interacts with and modulates the activity of target cytoplasmic proteins. This specificity resides in the structure of the interface between AGB1 and its targets. Important surface residues of AGB1, which were deduced from a comparative evolutionary approach, were mutated to dissect AGB1-dependent physiological functions. Analysis of the capacity of these mutants to complement well-established phenotypes of Gβ-null mutants revealed AGB1 residues critical for specific AGB1-mediated biological processes, including growth architecture, pathogen resistance, stomata-mediated leaf-air gas exchange, and possibly photosynthesis. These findings provide promising new avenues to direct the finely tuned engineering of crop yield and traits.

Heterotrimeric G-proteins are conserved signaling components across diverse eukaryote species (Jones and Assmann, 2004; Johnston et al., 2007; Jones et al., 2011a, 2011b). Upon perception of a cognate ligand by its seven-transmembrane receptor on the cell surface, the seven-transmembrane receptor-associated heterotrimeric G-protein complex dissociates to form an activated Gα-subunit and an obligate G$\beta\gamma$ dimer, which in turn trigger transient cellular changes by interacting with downstream proteins, typically enzymes, called effectors. In mammals, several Gα- and G$\beta\gamma$-interacting effectors were identified, including well-studied adenylyl cyclase 2, phospholipase C β2, and cation channels (Sunahara et al., 1996; Rhee and Bae, 1997; Schneider et al., 1997). None of these mammalian effectors are found in Arabidopsis (*Arabidopsis thaliana*; Jones and Assmann, 2004), although other potential effectors were proposed or shown (Klopffleisch et al., 2011). For example, physical interaction of the Arabidopsis Gα-subunit (AtGPA1) was shown for THYLAKOID FORMATION1 (THF1), an outer membrane protein on the plastid, which works with G proteins in sugar sensing and chloroplast development (Huang et al., 2006). Similarly, PHOSPHOLIPASE D ALPHA1 (PLDα1) and the cupin domain protein Atpirin1 may be important in AtGPA1 modulation of abscisic acid (ABA) signaling, an important component of plant morphogenesis and water use efficiency (Lapik and Kaufman, 2003; Mishra et al., 2006). A combination of approaches were exploited to identify physical (Klopffleisch et al., 2011) and genetic (Wang et al., 2006) interactors of Arabidopsis Gβ-subunit (AGB1). AGB1 interactors include N-MYC DOWNREGULATED-LIKE1 (NDL1) (Mudgil et al., 2009) and ACIREDUCTONE DIOXYGENASE1 (ARD1) (Friedman et al., 2011). ARD1

[1] This work was supported by the National Institute of General Medical Sciences (grant no. R01GM065989 to A.M.J.), the National Science Foundation (grant nos. MCB–0723515 and MCB–0718202 to A.M.J.), the Deutsche Forschungsgemeinschaft (grant no. SFB670 to R.P.), the Ministerio de Ciencia e Innovación (grant no. BIO2009–07161 to A.M. and a Ph.D. fellowship to M.D.-C.), the U.S. Department of Agriculture Agricultural Research Service (to F.L.B.), and the Division of Chemical Sciences, Geosciences, and Biosciences, Office of Basic Energy Sciences, U.S. Department of Energy (grant no. DE–FG02–05er15671 to A.M.J.).

* Corresponding author; e-mail alan_jones@unc.edu.

The author responsible for distribution of materials integral to the findings presented in this article in accordance with the policy described in the Instructions for Authors (www.plantphysiol.org) is: Alan M. Jones (alan_jones@unc.edu).

[W] The online version of this article contains Web-only data.

[OA] Open Access articles can be viewed online without a subscription.

www.plantphysiol.org/cgi/doi/10.1104/pp.112.196337

is the only confirmed plant Gβ effector to date (i.e. the only plant protein found so far whose enzymatic activity is directly modulated by a G protein; Friedman et al., 2011). The NDL1 protein has no known enzymatic function, although it resembles a lipase/esterase but lacks the critical catalytic triad. NDL1 and G-proteins work concertedly to control polar auxin transport streams in the root (Mudgil et al., 2009) and the inflorescence stem (Y. Mudgil and A.M. Jones, unpublished data). Mutants lacking NDL1 have reduced basipetal and increased acropetal transport of auxin and, as a consequence, lateral root development is altered. Consistent with NDL1 operating in the G-protein pathway, seedlings lacking GPA1 have less (whereas those lacking AGB1 have greater) root mass than wild-type seedlings, pointing to a role in the regulation of cell proliferation (Ullah et al., 2003; Chen et al., 2006). Other cell proliferation defects were characterized in G-protein mutants. For example, in the presence of 1% sucrose (Suc) or glucose (Glu), 50-h-old etiolated *agb1* seedlings display shorter hypocotyls and more open apical hooks, which is the consequence of reduced epidermal cell numbers in the hypocotyl (Ullah et al., 2003; Wang et al., 2006). *agb1* mutants also display an increased stomatal index and altered leaf, silique, and rosette morphologies (Ullah et al., 2003; Zhang et al., 2008; Booker et al., 2012).

From an agricultural perspective, the most significant phenotype of Arabidopsis and rice (*Oryza sativa*) G-protein mutants is the profound difference in innate immune responses. The Arabidopsis *agb1* null mutant shows reduced accumulation of reactive oxygen species (ROS) in response to microbial inducers such as bacterial flagellin and EF-Tu (Ishikawa, 2009). Moreover, *agb1* null mutants are hypersensitive to the necrotrophic fungi *Plectosphaerella cucumerina* and *Alternaria brassicicola* and the hemibiotrophic fungus *Fusarium oxysporum* (Llorente et al., 2005; Trusov et al., 2006, 2009; Delgado-Cerezo et al., 2012). Moreover, rice Gα mutants (*rga1*) are more susceptible to the rice blast fungus *Magnaporthe grisea* (Suharsono et al., 2002). The enhanced susceptibility of *agb1* mutants to *F. oxysporum* may result from the altered function of MYC2, a basic helix-loop-helix transcription factor regulating diverse jasmonate-dependent biological processes (Trusov et al., 2009). More recent data also suggest a link between AGB1-mediated *P. cucumerina* resistance and the modification of cell wall architecture (Delgado-Cerezo et al., 2012). Another important agricultural trait regulated by the heterotrimeric G protein is transpiration efficiency, which is increased in *gpa1* mutants (Nilson and Assmann, 2010). However, increased transpiration efficiency at high light levels in *gpa1* mutants is simply due to reduced stomatal density (Nilson and Assmann, 2010). GPA1 and AGB1 subunits modulate stomatal density antagonistically (Zhang et al., 2008; Booker et al., 2012).

Finally, and not surprisingly, signal transduction pathways of several phytohormones and environmental stimuli are altered in G-protein mutants, including ABA (Wang et al., 2001; Pandey and Assmann, 2004; Pandey et al., 2006), brassinosteroid (Ullah et al., 2002; Gao et al., 2008), auxin (Ullah et al., 2003), and red/far-red light (Wei et al., 2008; Botto et al., 2009), although not all phytochrome responses involve G proteins (Jones et al., 2003).

These myriad phenotypes may be a manifestation of the complexity of altered activity of targets downstream of G-protein activation. AtGPA1 activation occurs when GTP replaces GDP, resulting in a new protein conformation and an exposed surface on the Gβγ-subunit. Gβγ dimer activation occurs when it is released from the complex to expose new protein interfaces that were sequestered by Gα and other elements of the G-protein complex. We selected a limited but informative set of phenotypes as readouts for AGB1 signaling in a broad range of plant biology, including development, hormone physiology, plant immune responses, and disease resistance, as well as carbon dioxide (CO_2) assimilation and transpiration. To identify the active-state protein interfaces for each of these processes, we mutated a cluster of surface-exposed residues to determine which mutations disrupted signaling as interpreted through the inability to complement *agb1* mutant phenotypes upon transgenic expression of the mutant variants. The selection of mutations was based on phylogenetic and structural analyses for plant-specific surfaces that we originally tested to map the potential interface between an animal Gβ-subunit and its cognate target phospholipase β2 (Friedman et al., 2009). In essence, these are residues that while conserved in plants have evolved to become uniquely functional in mammals. Our purpose here is to determine what function these residues serve in plants. Specifically, we sought to distinguish different functions of AGB1 among many by observing which AGB1-dependent pathways are disrupted when these potential effector interfaces are mutated.

RESULTS

Mutant AGB1 Proteins Are Expressed and Properly Folded in the *agb1-2* Background

Residues on the AGB1-binding surface for mutagenesis analysis were selected and mutated as described before (Friedman et al., 2009). The residues selected were (1) located on the solvent-exposed surface area of the protein, (2) invariant between plants and mammals, and (3) not required for structural maintenance of the Gβγ dimer. Trp-109 and Ser-129 are both located in the Gα-binding domain, whereas the function of the interfaces containing either residues Glu-248 and Arg-25 or Gln-120, Thr-188, and Arg-235 is unknown. The conservation of residues on the AGB1 protein-binding interface suggests their functional importance in association with downstream effectors. Realizing that one Gβγ effector may share the same Gβ-interacting region with another, we hypothesized

that these four mutations may affect the binding of AGB1 to diverse effectors; therefore, the corresponding AGB1 mutants will only have partial function as compared with the wild type. Each mutant AGB1 variant, either with or without a 10× Myc tag, was expressed in the *agb1-2* background, and two to four independent nontagged and tagged transgenic lines per construct were selected for characterization (Fig. 1) and phenotyping (Figs. 2–5). We found that the phenotypes of both the 10× Myc-tagged and nontagged lines led to the same conclusions. For simplicity and clarity, results of the same set of tagged lines for each mutation are shown for the subsequent experiments. We found that all four *AGB1* mutants that code for protein variants were stably expressed (Fig. 1, middle panel). In addition, each GFP-tagged mutant was targeted to the plasma membrane (Fig. 1, bottom panel), thus revealing the expected AGB1 subcellular localization. Plasma membrane tethering of AGB1 depends on the formation of a heterodimer with the AGG1 subunit via its N-terminal coiled-coil motif (Obrdlik et al., 2000; Adjobo-Hermans et al., 2006). Therefore, proper plasma membrane localization of mutated AGB1 suggests a functional conformation. Further evidence of authentic protein conformation is provided by the fact that each mutant variant is capable of tightly interacting with its obligate AGG partner in vitro (Friedman et al., 2011). Finally, as described below, each mutant AGB1 was able to genetically complement at least one *agb1*-2 loss-of-function phenotype. Taken together, these results require that each AGB1 mutant was properly folded and localized in the plant cell.

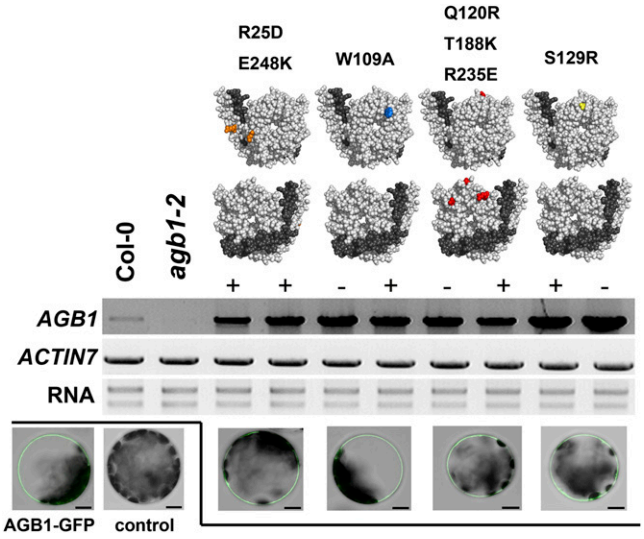

Figure 1. Site-directed mutagenesis of AGB1. The top panel shows the top and bottom views of AGB1 (light gray) and the closely associated Gγ-subunit (dark gray). Colored residues indicate point mutations generated. From left to right: R25D E248K, W109A, Q120R T188K R235E, and S129R. The middle panel shows the results of reverse transcription-PCR analysis of Myc-tagged (+) and nontagged (−) mutated *AGB1* expression in the transgenic lines used in this study. Total RNA was extracted from 10-d-old seedlings. PCR was repeated twice for each biological sample, and a total of two biological replicates were tested. *ACTIN7* was used as the loading control. Ethidium bromide-stained rRNAs (28S rRNA and 18S rRNA) are shown as a quality control for the RNA samples. The bottom panel shows the plasma membrane localization of mutant AGB1 proteins. Mesophyll protoplasts were isolated from 5-week-old Columbia (Col-0) plants and subsequently transfected with 20 μg of plasmids that allow transient expression of N-terminally GFP-tagged wild-type or mutated *AGB1*. Each image shows a single optical section focusing at the plasma membrane. GFP signal was not detected in untransfected (control) protoplasts. Bars = 10 μm.

Dissection of *agb1-2* Signaling in Development

Loss-of-function alleles of *AGB1* confer morphological alterations in vegetative and reproductive organs of Arabidopsis (Lease et al., 2001; Ullah et al., 2003), some of which are due to aberrant auxin transport (Mudgil et al., 2009). As a validation of our experimental approach, we first tested the phenotypic complementation of *agb1-2* by the yellow fluorescent protein/hemagglutinin-tagged wild-type AGB1. Our data (Supplemental Fig. S1), together with previous reports (Chen et al., 2006; Chakravorty et al., 2012), indicate that ectopic expression of *AGB1* rescues the developmental lesions of the *agb1* mutant without causing discernible side effects. We tested functional rescue of the *agb1-2* mutant by variant AGB1 proteins of selected developmental phenotypes that represent most stages in the life cycle of Arabidopsis. At 50 h, the etiolated *agb1-2* hypocotyls are shorter than the wild type (Wang et al., 2006). None of the mutated AGB1 proteins were able to fully rescue the hypocotyl to the wild-type length; however, W109A and S129R mutants partially rescued the hypocotyl phenotype (Fig. 2A). At 10 d, the lateral root density of *agb1-2* seedlings is higher than that of the wild type due to increased basipetal auxin transport (Mudgil et al., 2009). S129R AGB1 fully restored the lateral root density to the wild-type level, indicating that Ser-129 is not critical for the lateral root development. The other mutations conferred partial complementation of the lateral root phenotype (Fig. 2B). At 3 weeks, *agb1-2* leaves have a scorable leaf phenotype; the lamina is compact and rounded and the petiole is shorter (Ullah et al., 2003). Figure 2C shows that among the mutated AGB1 proteins, only plants expressing *W109A* and *S129R* had the wild-type leaf morphology. G-protein mutants have altered stomatal indices (Zhang et al., 2008; Nilson and Assmann, 2010; Booker et al., 2012). Just as for the lateral root phenotype, only S129R fully rescued the stomatal phenotype, whereas the other transgenic lines either had the *agb1-2* phenotype or were partially rescued (Fig. 2D). Finally, we scored a late-development phenotype. *agb1-2* siliques are shorter and wider than wild-type siliques and have a blunt tip (Ullah et al., 2003). The molecular mechanism underpinning this morphological change is unclear, although

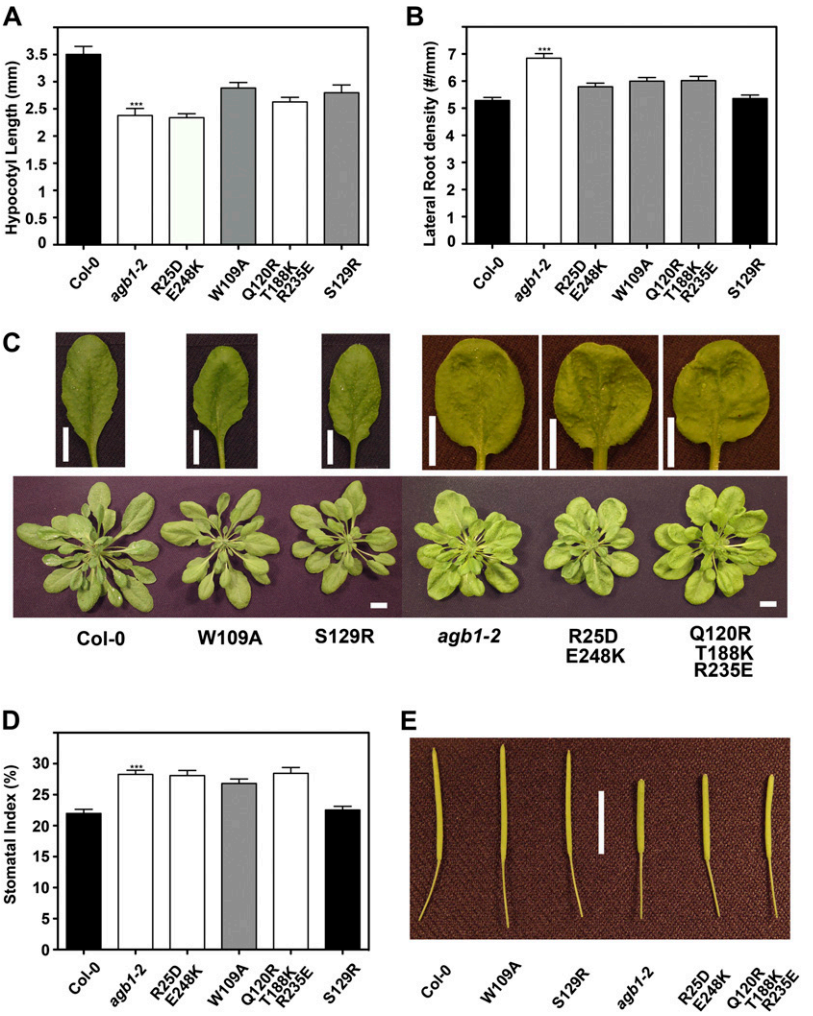

Figure 2. Analyses of developmental phenotypes in wild-type (Columbia [Col-0]), *agb1-2*, and transgenic plants. A, Hypocotyl length of 50-h-old etiolated seedlings ($n = 15$). B, Density of lateral roots (emergent lateral roots + lateral root primordia) of 10-d-old seedlings ($n = 30$). C, Morphological comparison of fully expanded rosette leaves and aerial parts of plants. D, Stomatal index on the abaxial epidermis of cotyledons from 9-d-old seedlings. E, Morphological comparison of mature siliques. The colors of bars indicate the extent to which a phenotype was rescued (black = wild type, gray = partially rescued, white = *agb1-2* like). Data for wild-type plants are plotted in black, and those for *agb1-2* mutants are plotted in white. All values are means ± SE, and assays were repeated two to four times with similar results. Asterisks indicate significant differences from wild-type plants (*** $P < 0.001$; Student's *t* test). Bars in C and E = 1 cm.

it is known that the AGB1/AGG3 dimer is an important modulator of reproductive organ shapes (Chakravorty et al., 2011; Li et al., 2012). We found that W109A and S129R fully rescued this reproductive phenotype, whereas the other two tested AGB1 mutants failed to restore the wild-type morphology (Fig. 2E). This indicates that residues Arg-25, Gln-120, Thr-188, Arg-235, and Glu-248 are critical for signaling several underlying morphologies.

Dissection of *agb1-2* Signaling in Hormone Physiology

The *agb1-2* mutant is hypersensitive to 6% Glc (Wang et al., 2006), implying a role of the heterotrimeric G protein in mediating sugar signal transduction. We examined functional rescue of the Glc-hypersensitive phenotype in the variant AGB1 transgenic lines. Just as for the hypocotyl-length phenotype (Fig. 2A), no AGB1 mutant was able fully to restore Glc sensitivity to the wild-type level, although the S129R variant showed a partial rescue (Fig. 3A). There was no discernible difference between the wild type and the *agb1* mutants for the osmotic control treatment (Supplemental Fig. S2). ABA, a key water deficiency-related phytohormone, inhibits lateral root development and drastically modulates root morphology under osmotic stress (De Smet et al., 2003, 2006). The *agb1-2* mutant is hypersensitive to ABA-inhibited lateral root development (Pandey et al., 2006). Seedlings were grown vertically on plates with or without ABA (Fig. 3B), and ABA-inhibited lateral root development in each transgenic line was compared with that of wild-type and *agb1-2* seedlings using two-way ANOVA (Fig. 3C). The ABA-hypersensitive phenotype was rescued fully by the S129R mutation and partially by the W109A mutation (Fig. 3C). In contrast, neither the double nor the triple mutants complemented this phenotype (Fig. 3C).

Dissection of *agb1-2* Signaling in flg22-Triggered ROS Production

The sensing of conserved microbe-associated molecular patterns such as bacterial flagellin or its elicitor-active peptide component, flg22, results in a series of stereotypic cellular responses that are thought to contribute to the activation of plant innate immune

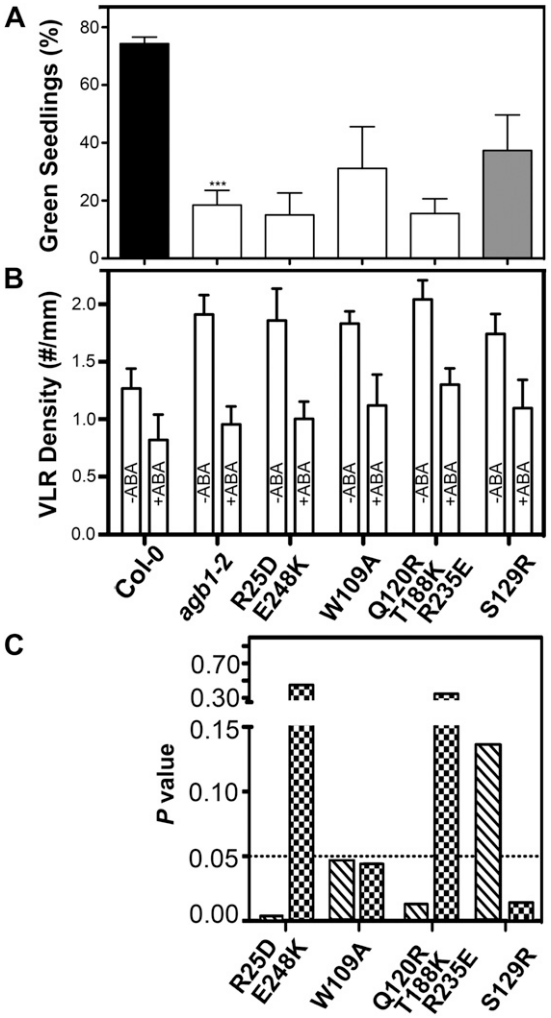

Figure 3. Analyses of Glc- and ABA-responsive phenotypes in wild-type (Columbia [Col-0]), *agb1-2*, and transgenic plants. A, Two percent (w/v) Glc-hypersensitive phenotype of *agb1-2* and of transgenic lines. The percentages of green seedlings were scored after 10 d of growth at 23°C. The experiment was repeated three times, and data were averaged. The colors of bars indicate the extent to which a phenotype was rescued (gray = partially rescued, white = *agb1-2* like). Data for wild-type plants are plotted in black, and those for *agb1-2* mutants are plotted in white. The error bars represent SD. Asterisks indicate significant differences from wild-type plants (*** $P < 0.001$; Student's *t* test). B and C, Inhibition of lateral root development by ABA. VLR, Visible lateral roots. The experiment was repeated three times, and data were averaged and are shown in B. The error bars represent SD. *P* values of ANOVA analyses are plotted in C. The hatched bars represent comparison of each transgenic line with wild-type plants, whereas the checkered bars represent comparison with *agb1-2* plants.

responses (Boller and Felix, 2009). These reactions comprise, among others, the influx of calcium (Ca^{2+}) ions from the apoplastic space, the extracellular accumulation of ROS, and the intracellular activation of mitogen-associated protein kinase cascades (Boller and Felix, 2009). Microbe-associated molecular pattern-induced formation of hydrogen peroxide is severely compromised in *agb1-2* mutant plants (Ishikawa, 2009), suggesting a link between AGB1 function and ROS accumulation. We exploited this phenotype to assess the capability of AGB1 mutant variants to complement the *agb1* deficiency in ROS production. The W109A mutant completely restored, whereas the S129R single, the R25D E248K double, and the Q120R T188K R235E triple mutants partially restored flg22-triggered ROS formation in the *agb1-2* background (Fig. 4). In the case of the W109A, S129R, and Q120R T188K R235E variants, these results were corroborated

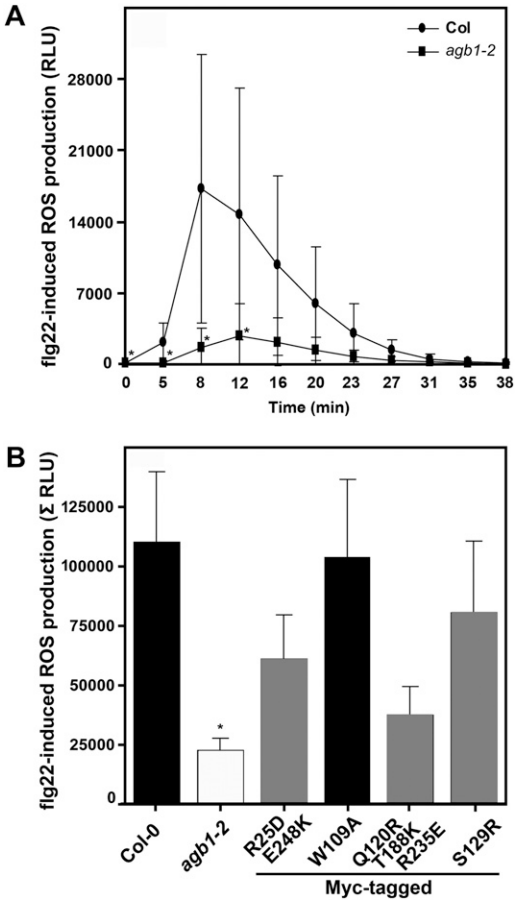

Figure 4. Accumulation of ROS after flg22 treatment. Leaf discs from 4- to 5-week-old plants were treated with 1 μM flg22, and ROS formation was measured as relative light units (RLU) in a chemiluminescence assay during a time course of 38 min after flg22 application. A, Representative response curves of wild-type (Columbia [Col-0]) and *agb1*-2 mutant plants. Data represent means ± SD of at least six leaf discs per genotype. B, flg22-induced ROS production in the indicated genotypes is represented as the integrated area under the ROS curve measured and is referred to as Σ RLU. The colors of bars indicate the extent to which a phenotype was rescued (black = wild type, gray = partially rescued). Data for wild-type plants are plotted in black, and those for *agb1-2* mutants are plotted in white. Results are presented as means ± SE of at least four independent experiments with four to 12 leaf discs per genotype. Asterisks indicate significant differences from wild-type plants (* $P < 0.05$; Student's *t* test).

by measurements with additional independent transgenic lines (Supplemental Fig. S3).

Dissection of *agb1-2* Signaling in Agricultural Traits

Compared with wild-type plants, *agb1* null mutants are substantially more susceptible to the pathogenic fungi *F. oxysporum* (f. sp. *conglutinans*) and *P. cucumerina* (Llorente et al., 2005; Trusov et al., 2006, 2007). Soil-borne *F. oxysporum* hyphae enter plant roots and then spread through the vascular system. The infection results in root and leaf growth inhibition, anthocyanin accumulation, chlorosis, and finally plant decay (Agrios, 2005). We scored the leaf chlorosis phenotype 8 to 9 d after inoculation. The lines expressing the variant *Q120R T188K R235E* were as susceptible to *F. oxysporum* as *agb1-2*, whereas the lines expressing *W109A* or *S129R* were similar to the wild type (Fig. 5A). The lines expressing *R25D E248K* showed a partial complementation of *F. oxysporum* hypersusceptibility displayed in *agb1-2* (Fig. 5A). These data indicate that Trp-109 and Ser-129 are not critical for AGB1-mediated fungal resistance, whereas residues Arg-25, Gln-120, Thr-188, Arg-235, and Glu-248 are required for the defense response to *F. oxysporum*. The same results were obtained for *P. cucumerina* susceptibility (Fig. 5B), suggesting that AGB1 may utilize at least overlapping sets of effectors to elicit the Arabidopsis defense response against all necrotic fungi.

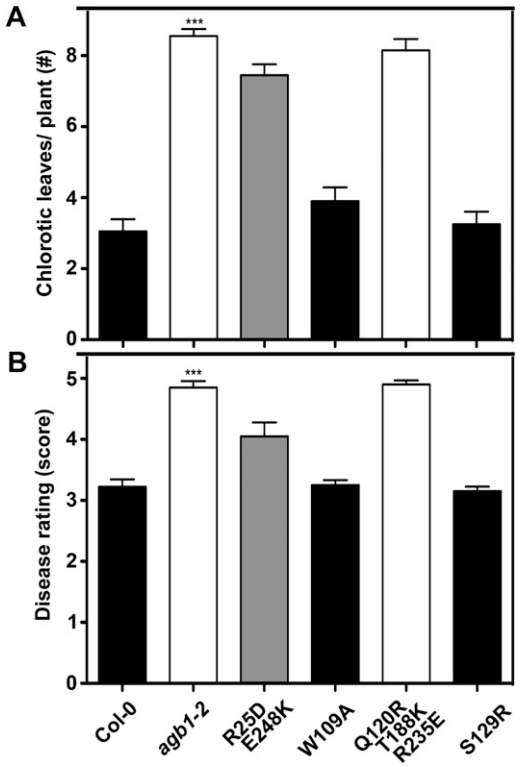

Figure 5. Susceptibility to necrotrophic fungi in wild type (Columbia [Col-0]), *agb1-2*, and transgenic plants. A, Number of yellow-veined leaves per infected plant. A total of 20 plants for each line were inoculated with *F. oxysporum* spores. Chlorotic leaves were counted 8 to 9 d after infection. B, Disease rating scores 11 d after inoculation with 2×10^6 spores mL^{-1} *P. cucumerina*. The colors of bars indicate the extent to which a phenotype was rescued (black = wild type, gray = partially rescued, white = *agb1-2* like). Data for wild-type plants are plotted in black, and those for *agb1-2* mutants are plotted in white. All values are means ± SE, and data are from one of three independent experiments with the same conclusion. Asterisks indicate significant differences from wild-type plants (*** $P < 0.001$; Student's *t* test).

The heterotrimeric G protein mediates epidermal cell patterning (Zhang et al., 2008) and therefore genetically controls transpiration efficiency at the level of stomatal density (Nilson and Assmann, 2010). We performed gas-exchange analysis to determine whether steady-state net photosynthesis and stomatal conductance along a gradient of light intensities are affected by the *agb1* null mutation at ambient CO_2 level (approximately 400 μmol mol^{-1}). We did not detect a significant change in photosynthetic rate or stomatal conductance for the full set of *agb1-2* mutant or wild-type leaves under our experimental conditions (Supplemental Fig. S4; data not shown). Photosynthesis is influenced by multiple environmental factors such as light intensity, CO_2 levels, and vapor pressure deficit. As shown in Supplemental Figure S4, increasing photosynthesis rate and conductance increase with light intensity. Stomatal aperture is affected, in part, by signaling through G-proteins. Stomatal aperture is greater in *gpa1* mutants than in the wild type at high light. We speculate that under certain conditions of [CO_2] and light, stomatal aperture is compensating for differences in stomatal index.

DISCUSSION

Upon activation, both Gα- and G$\beta\gamma$-subunits of the heterotrimeric complex trigger intracellular signal transduction and amplification via physical association with specific effectors. The functional importance of the G$\beta\gamma$-effector interaction constrains the evolution of critical residues on the interface of Gβ proteins (Friedman et al., 2009). Through bioinformatic and phylogenetic analysis, we predicted that several surface residues are requisite for specific binding of AGB1 to one of its effectors, and we validated this prediction using an in vitro enzymatic assay (Friedman et al., 2011). Here, we examined the functional complementation of Gβ-null mutant phenotypes (Table S1) by transforming *agb1-2* with mutated *AGB1* variants, with the expectation of mapping candidate surface residues within interfaces between AGB1 and its unknown effectors involved in specific physiological processes. We found that the double and triple mutants were functionally impaired in rescuing most of the *agb1* phenotypes, indicating that residues Arg-25, Gln-120, Thr-188, Arg-235, and Glu-248 of AGB1 are critical for overlapping functions. Also, the data suggest that some residues may form common interfaces for the

binding of diverse effectors. The W109A mutant rescued some of the loss-of-function phenotypes but failed to complement others (Figs. 2–5), suggesting that a mutation can alter the regulation of some specific effectors without affecting other AGB1-mediated functions. The S129R mutation had a minor effect on AGB1 function and therefore may not be within any effector interface or is within an effector interface that operates in an untested pathway.

An interesting observation is that mutations W109A and S129R made on the Gα-binding surface had less effect than expected, because these amino acids reside in the Gα-Gβ protein-protein interface. An intensive mutational analysis on the conserved AGB1 surface for Gα association demonstrated that this region may not be critical for effector binding in plants (Chakravorty et al., 2012). This phenomenon is significantly different from retinal Gβ (Gβ1), in which mutations in the Gα-binding regions cause impaired activation of an array of effectors like phospholipases, adenylyl cyclases, and ion channels (Ford et al., 1998).

The pleiotropic actions of G-protein subunits limit their use as complete loss-of-function targets for breeding. For example, the rice *d1* mutant, which carries a null mutation of *RGA1*, the rice Gα subunit, is dwarf and consequently less likely to lodge (Fujisawa et al., 1999). However, the same genetic lesion in *RGA1* confers smaller seed size (Fujisawa et al., 1999) and less resistance to the blast fungus *Magnaporthe grisea* (Suharsono et al., 2002), both dramatically decreasing yield. A decrease in the rice Gβ-subunit reduces cell proliferation and confers seed sterility (Utsunomiya et al., 2011). Taken together with the data on AGB1 shown here, genetic ablation of G-protein complex proteins confers a wide set of traits, some beneficial and some not beneficial to agriculture.

While the work here is proof of concept, the observations point to a possible means to improve yield in rice. Just as for *rga1*, loss of the Gβ-subunit in rice confers dwarfness (Utsunomiya et al., 2011), an early trait found during the Green Revolution period that doubled rice yield simply by increasing harvest index (Weber and Fehr, 1966). Unfortunately, this Gβ-subunit mutant also has smaller seed and increased susceptibility to fungus. In Arabidopsis, the W109A mutant fully restored silique morphology, flg22-triggered ROS production, and fungal pathogen resistance to wild-type levels, but this mutation only partially rescued the shorter hypocotyl phenotype (Figs. 3 and 5). This indicates that residue Trp-109 of AGB1 is critical for the binding of effectors mediating cell division. We propose that the equivalent residue of rice Gβ could be mutated in order to generate a partially functioning Gβ-subunit, one having wild-type resistance to rice blast fungus yet, due to reduced cell division, would be dwarf and provide a higher harvest index.

In summary, we identified multiple sites on the AGB1 protein surface for functional significance in G-protein signaling. Our work provides fundamental knowledge to direct the finely tuned engineering of crop traits.

MATERIALS AND METHODS

Plant Material and Growth Conditions

The Arabidopsis (*Arabidopsis thaliana*) ecotype used in this study was Columbia. The *agb1-2* mutant was previously described (Ullah et al., 2003). The entire coding sequence of mutated *AGB1* (Friedman et al., 2011) was cloned into the pENTR/D-TOPO vector (Invitrogen) and subsequently shuttled in Gateway-based pGWB2 (no tag) and pGWB21 (N-terminal 10× Myc tag) vectors (Nakagawa et al., 2007) under the control of the cauliflower mosaic virus 35S promoter. To generate transgenic lines stably expressing *AGB1* mutants in the Gβ-null background, the binary constructs in the pGWB backbone were introduced into *Agrobacterium tumefaciens* GV3101 pMP90 by electroporation and then into the *agb1-2* mutant by floral dipping (Clough and Bent, 1998). All transgenic plants were selected on one-half-strength Murashige and Skoog (MS) medium containing 25 mg L^{-1} hygromycin. Suitable progeny homozygous for the respective transgene were used for all experiments.

Transcription Analysis

Total RNA was extracted from 10-d-old Arabidopsis seedlings using the RNeasy Plant Mini Kit (Qiagen). The first-strand complementary DNA (cDNA) was generated by use of the SuperScript II reverse transcriptase (Invitrogen) according to the manufacturer's instructions. For each sample, 1 μg of total RNA was reverse transcribed to produce first-strand cDNA. Full-length wild-type or mutated *AGB1* transcripts were amplified using primers AGB1 5′ primer (5′-CACCATGTCTGTCTCCGAG-3′) and AGB1 3′ primer (5′-TCAAATCACTCTCCTGTGTCCTCC-3′). *ACTIN7* transcripts were amplified as an internal control using primers Act-RT_for (5′-TGTTCCCAAGTATTGTTGGTCGTC-3′) and Act-RT_rev (5′-TGCTGAGGGATGCAAGGATTGATC-3′).

Preparation and Transient Transfection of Arabidopsis Protoplasts

To examine the subcellular localization of wild-type and mutated AGB1, the full-length cDNA fragment in the pENTR plasmid was subcloned into the Gateway-based pK7WGF2 vector (Karimi et al., 2002). The GFP fusion constructs were delivered into Arabidopsis mesophyll protoplasts (approximately 5×10^4 protoplasts per transfection) as described (Yoo et al., 2007). After incubation in 1 mL of W5 solution (154 mM NaCl, 125 mM $CaCl_2$, 5 mM KCl, 5 mM Glc, and 2 mM MES, pH 5.7) with 1% bovine serum albumin at room temperature for 16 h, the subcellular localization of GFP-tagged AGB1 (wild type or mutant) was visualized using a Zeiss 710 laser-scanning confocal microscope with a 40× oil-immersion quartz, apochromatic objective.

Morphologies

In-plate assays were performed using one-half-strength MS basal salts, 1% Suc, and 0.8% phytoagar (Research Products International). Sterilized seeds were sown and stratified for 2 d before being moved to the growth chamber at 23°C. For hypocotyl length assays, seeds were pretreated with light (200 μmol m^{-2} s^{-1}) for 2 h and then incubated in the dark for 50 h. Etiolated seedlings on plates were imaged and hypocotyl lengths were measured with the publicly available ImageJ software (http://rsbweb.nih.gov/ij/). Stomatal index was determined as described previously (Zhang et al., 2008) except that seedlings were stained with 1 mg mL^{-1} propidium iodine for 15 min and rinsed briefly with distilled, deionized water before visualization with a Zeiss 710 laser-scanning confocal microscope. To examine the development of lateral roots, 10-d-old, vertically grown seedlings were fixed in 100% formalin-acetic acid-alcohol with Eosin Y overnight at 4°C. The fixed seedlings were cleared with 95% ethanol, rinsed with distilled, deionized water, and subsequently stained with 100% acetocarmine solution (Carolina Biological Supply) as described (Enstone et al., 2001). Red patches represent lateral root primordia.

The morphology of rosette leaves and siliques was determined as described (Boyes et al., 2001; Ullah et al., 2003). Arabidopsis plants were grown in soil under a short-day regime (8 h of light/16 h of dark). The fully expanded

rosette leaves at stage 5.10 and mature siliques at stage 6.50 were detached from the plants for imaging.

Measurements of Responsive Traits

To observe the effect of exogenous Glc on plant growth, seeds were germinated on a low-Glc (2%) medium containing nitrogen as KNO_3 (1.9 g L^{-1}) and NH_4NO_3 (1.65 g L^{-1}) as described previously (Cho et al., 2010). Seedlings showing chlorosis were scored as Glc sensitive. To examine transient Glc signaling in plants, changes in *TBL26* transcript level in response to sugar treatment were checked using real-time PCR as described previously (Grigston et al., 2008). To study the inhibitory effect of ABA on lateral root development, seeds were germinated vertically on one-half-strength MS medium solidified with 0.5% (w/v) phytagel (Sigma-Aldrich). A homogenous subset of 4-d-old seedlings was transferred to control (0.1% [v/v] ethanol) or treatment (10^{-6} μM ABA) plates and grown under the same conditions for an additional 5 d before the density of visible lateral roots was measured.

Gas-Exchange Measurements

Photosynthesis and stomatal conductance were measured with an open gas-exchange system (LI-6400; LI-COR) as described by Rosenthal et al. (2011). Plants were taken out from growth chambers, immediately placed in the cuvette of the gas-exchange system, and allowed to reach steady-state photosynthesis at their growth ($[CO_2]$; approximately 400 μmol mol^{-1}) at the indicated light levels. For measuring photosynthesis, the initial leaf chamber conditions were set to a constant leaf temperature of 23.26°C ± 0.24°C, the leaf vapor pressure deficit was 0.82 ± 0.133 kPa, and the chamber relative humidity was 70.75% ± 5.1%. Leaves in chambers remained under constant conditions for a minimum of 10 min prior to recording steady-state net photosynthesis and stomatal conductance. For measuring stomatal conductance, the leaf chamber conditions were set to a constant leaf temperature of 23°C ± 0.20°C, the leaf vapor pressure deficit was 1.19 ± 0.08 kPa, and the chamber relative humidity was 58% ± 1.0%.

Measurement of flg22-Induced ROS Accumulation

ROS assays were performed as described previously (Gómez-Gómez et al., 1999) with the following modifications: leaf discs (5 mm diameter) excised from 4- to 5-week old plants were incubated overnight in water and then transferred into microtiter plates containing 50 μL of water. ROS production was triggered by the addition of 1 μM flg22 peptide (QRLSTGSRINSAKDDAAGLQIA; synthesized by Centic Biotec) applied in a reaction mixture containing 50 μL of water, 20 μM luminol (Sigma-Aldrich), and 1 μg of horseradish peroxidase (Sigma-Aldrich). Luminescence was measured in a Centro LB 960 microplate luminometer (Berthold Technologies) during a time course of 38 min after flg22 application.

Pathogen Infection Assays

For *Fusarium oxysporum* resistance assays, 2-week-old Arabidopsis seedlings grown in soil (California University mix) were uprooted, briefly rinsed with water, and incubated in *Fusarium* spore solution for 30 to 60 s. After inoculation, the seedlings were replanted into fresh soil and grown at 28°C to 30°C. Leaves with yellow veins were counted 8 to 9 d after inoculation. *F. oxysporum* spore solution was prepared as described previously (Trusov et al., 2006). To examine susceptibility to the necrotrophic fungus *Plectosphaerella cucumerina*, 3-week-old soil-grown plants were inoculated with a suspension of 2×10^6 mL^{-1} spores as described previously (Berrocal-Lobo et al., 2002). The progress of disease symptoms was scored 11 d after infection according to the following scheme: 0, plant is completely healthy; 1, some yellow spots can be observed; 2, there are one or two leaves dead; 3, there are over three dead leaves; 4, few tissues remain green; 5, plant completely dead.

Statistical Analyses

Statistical analyses were performed using GraphPad Prism 5. Experimental data were analyzed with Student's *t* test and two-way ANOVA.

Sequence data from this article can be found in the GenBank/EMBL data libraries under accession numbers At4g34460 (*AGB1*).

Supplemental Data

The following materials are available in the online version of this article.

Supplemental Figure S1. Phenotypic analysis of the *35S:AGB1-YFP-HA/agb1-2* complementation line.

Supplemental Figure S2. Osmotic control for the Glc-sensing assay.

Supplemental Figure S3. Accumulation of ROS after flg22 treatment.

Supplemental Figure S4. Gas-exchange analysis of wild-type, *agb1-2*, and transgenic plants under different light intensities.

Supplemental Table S1. Confidence levels for statistical differences in genotype-dependent phenotypes.

ACKNOWLEDGMENTS

A. Frick-Cheng thanks the National Science Foundation for a SURE fellowship and E. Friedman for mentoring.

Received February 24, 2012; accepted May 3, 2012; published May 8, 2012.

LITERATURE CITED

Adjobo-Hermans MJ, Goedhart J, Gadella TW Jr (2006) Plant G protein heterotrimers require dual lipidation motifs of Gα and Gγ and do not dissociate upon activation. J Cell Sci **119:** 5087–5097

Agrios GN (2005) Plant Pathology, Ed 5. Elsevier Academic Press, New York

Berrocal-Lobo M, Molina A, Solano R (2002) Constitutive expression of ETHYLENE-RESPONSE-FACTOR1 in Arabidopsis confers resistance to several necrotrophic fungi. Plant J **29:** 23–32

Boller T, Felix G (2009) A renaissance of elicitors: perception of microbe-associated molecular patterns and danger signals by pattern-recognition receptors. Annu Rev Plant Biol **60:** 379–406

Booker FL, Burkey KO, Morgan PM, Fiscus EL, Jones AM (2012) Minimal influence of G-protein null mutations on ozone-induced changes in gene expression, foliar injury, gas exchange and peroxidase activity in *Arabidopsis thaliana* L. Plant Cell Environ **35:** 668–681

Botto JF, Ibarra S, Jones AM (2009) The heterotrimeric G-protein complex modulates light sensitivity in Arabidopsis thaliana seed germination. Photochem Photobiol **85:** 949–954

Boyes DC, Zayed AM, Ascenzi R, McCaskill AJ, Hoffman NE, Davis KR, Görlach J (2001) Growth stage-based phenotypic analysis of *Arabidopsis*: a model for high throughput functional genomics in plants. Plant Cell **13:** 1499–1510

Chakravorty D, Trusov Y, Botella JR (2012) Site-directed mutagenesis of the Arabidopsis heterotrimeric G protein beta subunit suggests divergent mechanisms of effector activation between plant and animal G proteins. Planta **235:** 615–627

Chakravorty D, Trusov Y, Zhang W, Acharya BR, Sheahan MB, McCurdy DW, Assmann SM, Botella JR (2011) An atypical heterotrimeric G-protein γ-subunit is involved in guard cell K-channel regulation and morphological development in Arabidopsis thaliana. Plant J **67:** 840–851

Chen JG, Gao Y, Jones AM (2006) Differential roles of Arabidopsis heterotrimeric G-protein subunits in modulating cell division in roots. Plant Physiol **141:** 887–897

Cho YH, Sheen J, Yoo SD (2010) Low glucose uncouples hexokinase1-dependent sugar signaling from stress and defense hormone abscisic acid and C_2H_4 responses in Arabidopsis. Plant Physiol **152:** 1180–1182

Clough SJ, Bent AF (1998) Floral dip: a simplified method for Agrobacterium-mediated transformation of Arabidopsis thaliana. Plant J **16:** 735–743

Delgado-Cerezo M, Sánchez-Rodríguez C, Escudero V, Miedes E, Fernández PV, Jordá L, Hernández-Blanco C, Sánchez-Vallet A, Bednarek P, Schulze-Lefert P, et al (2012) Arabidopsis heterotrimeric G-protein regulates cell wall defense and resistance to necrotrophic fungi. Mol Plant **5:** 98–114

De Smet I, Signora L, Beeckman T, Inzé D, Foyer CH, Zhang H (2003) An abscisic acid-sensitive checkpoint in lateral root development of Arabidopsis. Plant J **33:** 543–555

De Smet I, Zhang H, Inzé D, Beeckman T (2006) A novel role for abscisic acid emerges from underground. Trends Plant Sci **11:** 434–439

Enstone DE, Peterson CA, Hallgren SW (2001) Anatomy of seedling tap roots of loblolly pine (*Pinus taeda* L.). Trees **15:** 98–111

Ford CE, Skiba NP, Bae H, Daaka Y, Reuveny E, Shekter LR, Rosal R, Weng G, Yang CS, Iyengar R, et al (1998) Molecular basis for interactions of G protein betagamma subunits with effectors. Science **280:** 1271–1274

Friedman EJ, Temple BR, Hicks SN, Sondek J, Jones CD, Jones AM (2009) Prediction of protein-protein interfaces on G-protein beta subunits reveals a novel phospholipase C beta2 binding domain. J Mol Biol **392:** 1044–1054

Friedman EJ, Wang HX, Jiang K, Perovic I, Deshpande A, Pochapsky TC, Temple BR, Hicks SN, Harden TK, Jones AM (2011) Acireductone dioxygenase 1 (ARD1) is an effector of the heterotrimeric G protein beta subunit in Arabidopsis. J Biol Chem **286:** 30107–30118

Fujisawa Y, Kato T, Ohki S, Ishikawa A, Kitano H, Sasaki T, Asahi T, Iwasaki Y (1999) Suppression of the heterotrimeric G protein causes abnormal morphology, including dwarfism, in rice. Proc Natl Acad Sci USA **96:** 7575–7580

Gao Y, Wang S, Asami T, Chen JG (2008) Loss-of-function mutations in the Arabidopsis heterotrimeric G-protein alpha subunit enhance the developmental defects of brassinosteroid signaling and biosynthesis mutants. Plant Cell Physiol **49:** 1013–1024

Gómez-Gómez L, Felix G, Boller T (1999) A single locus determines sensitivity to bacterial flagellin in Arabidopsis thaliana. Plant J **18:** 277–284

Grigston JC, Osuna D, Scheible WR, Liu C, Stitt M, Jones AM (2008) D-Glucose sensing by a plasma membrane regulator of G signaling protein, AtRGS1. FEBS Lett **582:** 3577–3584

Huang J, Taylor JP, Chen JG, Uhrig JF, Schnell DJ, Nakagawa T, Korth KL, Jones AM (2006) The plastid protein THYLAKOID FORMATION1 and the plasma membrane G-protein GPA1 interact in a novel sugar-signaling mechanism in *Arabidopsis*. Plant Cell **18:** 1226–1238

Ishikawa A (2009) The Arabidopsis G-protein β-subunit is required for defense response against *Agrobacterium tumefaciens*. Biosci Biotechnol Biochem **73:** 47–52

Johnston CA, Taylor JP, Gao Y, Kimple AJ, Grigston JC, Chen JG, Siderovski DP, Jones AM, Willard FS (2007) GTPase acceleration as the rate-limiting step in Arabidopsis G protein-coupled sugar signaling. Proc Natl Acad Sci USA **104:** 17317–17322

Jones AM, Assmann SM (2004) Plants: the latest model system for G-protein research. EMBO Rep **5:** 572–578

Jones AM, Ecker JR, Chen JG (2003) A reevaluation of the role of the heterotrimeric G protein in coupling light responses in Arabidopsis. Plant Physiol **131:** 1623–1627

Jones JC, Duffy JW, Machius M, Temple BR, Dohlman HG, Jones AM (2011a) The crystal structure of a self-activating G protein alpha subunit reveals its distinct mechanism of signal initiation. Sci Signal **4:** ra8

Jones JC, Temple BR, Jones AM, Dohlman HG (2011b) Functional reconstitution of an atypical G protein heterotrimer and regulator of G protein signaling protein (RGS1) from Arabidopsis thaliana. J Biol Chem **286:** 13143–13150

Karimi M, Inzé D, Depicker A (2002) GATEWAY vectors for Agrobacterium-mediated plant transformation. Trends Plant Sci **7:** 193–195

Klopffleisch K, Phan N, Augustin K, Bayne RS, Booker KS, Botella JR, Carpita NC, Carr T, Chen JG, Cooke TR, et al (2011) Arabidopsis G-protein interactome reveals connections to cell wall carbohydrates and morphogenesis. Mol Syst Biol **7:** 532

Lapik YR, Kaufman LS (2003) The *Arabidopsis* cupin domain protein AtPirin1 interacts with the G protein α-subunit GPA1 and regulates seed germination and early seedling development. Plant Cell **15:** 1578–1590

Lease KA, Wen J, Li J, Doke JT, Liscum E, Walker JC (2001) A mutant *Arabidopsis* heterotrimeric G-protein β subunit affects leaf, flower, and fruit development. Plant Cell **13:** 2631–2641

Li S, Liu Y, Zheng L, Chen L, Li N, Corke F, Lu Y, Fu X, Zhu Z, Bevan MW, et al (2012) The plant-specific G protein γ subunit AGG3 influences organ size and shape in Arabidopsis thaliana. New Phytol **194:** 690–703

Llorente F, Alonso-Blanco C, Sánchez-Rodriguez C, Jorda L, Molina A (2005) ERECTA receptor-like kinase and heterotrimeric G protein from Arabidopsis are required for resistance to the necrotrophic fungus *Plectosphaerella cucumerina*. Plant J **43:** 165–180

Mishra G, Zhang W, Deng F, Zhao J, Wang X (2006) A bifurcating pathway directs abscisic acid effects on stomatal closure and opening in Arabidopsis. Science **312:** 264–266

Mudgil Y, Uhrig JF, Zhou J, Temple B, Jiang K, Jones AM (2009) *Arabidopsis* N-MYC DOWNREGULATED-LIKE1, a positive regulator of auxin transport in a G protein-mediated pathway. Plant Cell **21:** 3591–3609

Nakagawa T, Kurose T, Hino T, Tanaka K, Kawamukai M, Niwa Y, Toyooka K, Matsuoka K, Jinbo T, Kimura T (2007) Development of series of Gateway binary vectors, pGWBs, for realizing efficient construction of fusion genes for plant transformation. J Biosci Bioeng **104:** 34–41

Nilson SE, Assmann SM (2010) The α-subunit of the Arabidopsis heterotrimeric G protein, GPA1, is a regulator of transpiration efficiency. Plant Physiol **152:** 2067–2077

Obrdlik P, Neuhaus G, Merkle T (2000) Plant heterotrimeric G protein β subunit is associated with membranes via protein interactions involving coiled-coil formation. FEBS Lett **476:** 208–212

Pandey S, Assmann SM (2004) The *Arabidopsis* putative G protein-coupled receptor GCR1 interacts with the G protein α subunit GPA1 and regulates abscisic acid signaling. Plant Cell **16:** 1616–1632

Pandey S, Chen JG, Jones AM, Assmann SM (2006) G-protein complex mutants are hypersensitive to abscisic acid regulation of germination and postgermination development. Plant Physiol **141:** 243–256

Rhee SG, Bae YS (1997) Regulation of phosphoinositide-specific phospholipase C isozymes. J Biol Chem **272:** 15045–15048

Rosenthal DM, Locke AM, Khozaei M, Raines CA, Long SP, Ort DR (2011) Over-expressing the $C_{(3)}$ photosynthesis cycle enzyme Sedoheptulose-1-7 Bisphosphatase improves photosynthetic carbon gain and yield under fully open air $CO_{(2)}$ fumigation (FACE). BMC Plant Biol **11:** 123

Schneider T, Igelmund P, Hescheler J (1997) G protein interaction with K^+ and Ca^{2+} channels. Trends Pharmacol Sci **18:** 8–11

Suharsono U, Fujisawa Y, Kawasaki T, Iwasaki Y, Satoh H, Shimamoto K (2002) The heterotrimeric G protein α subunit acts upstream of the small GTPase Rac in disease resistance of rice. Proc Natl Acad Sci USA **99:** 13307–13312

Sunahara RK, Dessauer CW, Gilman AG (1996) Complexity and diversity of mammalian adenylyl cyclases. Annu Rev Pharmacol Toxicol **36:** 461–480

Trusov Y, Rookes JE, Chakravorty D, Armour D, Schenk PM, Botella JR (2006) Heterotrimeric G proteins facilitate Arabidopsis resistance to necrotrophic pathogens and are involved in jasmonate signaling. Plant Physiol **140:** 210–220

Trusov Y, Rookes JE, Tilbrook K, Chakravorty D, Mason MG, Anderson D, Chen JG, Jones AM, Botella JR (2007) Heterotrimeric G protein γ subunits provide functional selectivity in G$\beta\gamma$ dimer signaling in *Arabidopsis*. Plant Cell **19:** 1235–1250

Trusov Y, Sewelam N, Rookes JE, Kunkel M, Nowak E, Schenk PM, Botella JR (2009) Heterotrimeric G proteins-mediated resistance to necrotrophic pathogens includes mechanisms independent of salicylic acid-, jasmonic acid/ethylene- and abscisic acid-mediated defense signaling. Plant J **58:** 69–81

Ullah H, Chen JG, Temple B, Boyes DC, Alonso JM, Davis KR, Ecker JR, Jones AM (2003) The β-subunit of the *Arabidopsis* G protein negatively regulates auxin-induced cell division and affects multiple developmental processes. Plant Cell **15:** 393–409

Ullah H, Chen JG, Wang S, Jones AM (2002) Role of a heterotrimeric G protein in regulation of Arabidopsis seed germination. Plant Physiol **129:** 897–907

Utsunomiya Y, Samejima C, Takayanagi Y, Izawa Y, Yoshida T, Sawada Y, Fujisawa Y, Kato H, Iwasaki Y (2011) Suppression of the rice heterotrimeric G protein β-subunit gene, RGB1, causes dwarfism and browning of internodes and lamina joint regions. Plant J **67:** 907–916

Wang HX, Weerasinghe RR, Perdue TD, Cakmakci NG, Taylor JP, Marzluff WF, Jones AM (2006) A Golgi-localized hexose transporter is involved in heterotrimeric G protein-mediated early development in Arabidopsis. Mol Biol Cell **17:** 4257–4269

Wang XQ, Ullah H, Jones AM, Assmann SM (2001) G protein regulation of ion channels and abscisic acid signaling in Arabidopsis guard cells. Science **292:** 2070–2072

Weber CR, Fehr WR (1966) Seed yield losses from lodging and combine harvesting in soybeans. Agron J **58:** 287–289

Wei Q, Zhou W, Hu G, Wei J, Yang H, Huang J (2008) Heterotrimeric G-protein is involved in phytochrome A-mediated cell death of Arabidopsis hypocotyls. Cell Res **18:** 949–960

Yoo SD, Cho YH, Sheen J (2007) Arabidopsis mesophyll protoplasts: a versatile cell system for transient gene expression analysis. Nat Protoc **2:** 1565–1572

Zhang L, Hu G, Cheng Y, Huang J (2008) Heterotrimeric G protein α and β subunits antagonistically modulate stomatal density in Arabidopsis thaliana. Dev Biol **324:** 68–75

Figure S1

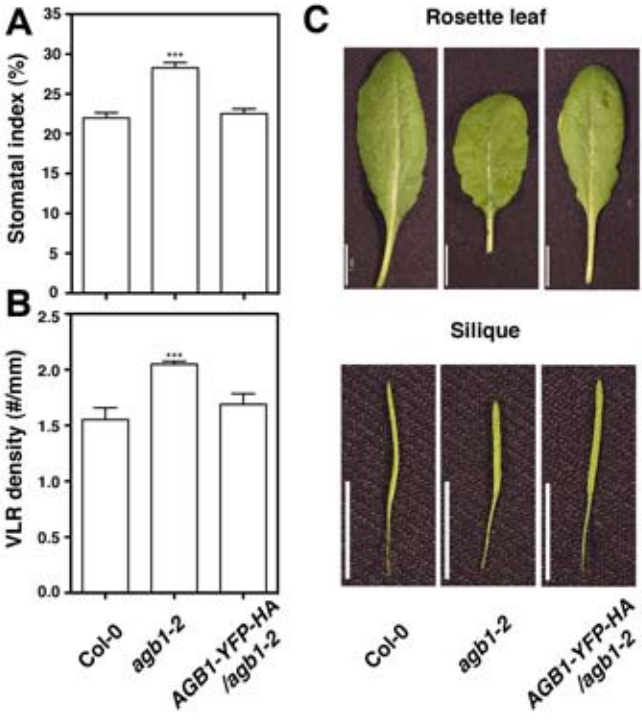

Figure S1. Phenotypic analysis on the *35S:AGB1-YFP-HA/agb1-2* complementation line.

A, Stomatal index on the abaxial epidermis of cotyledons from 9-day-old seedlings (n=20). B, Density of visible lateral roots (VLR) of 10-day-old seedlings (n=30). C, Comparison of fully expanded rosette leaves and siliques of plants. Values in A and B are mean ±SE. *Significant difference from wild-type plants (*** $p<0.001$). Scale bars in C = 1 cm.

Figure S2

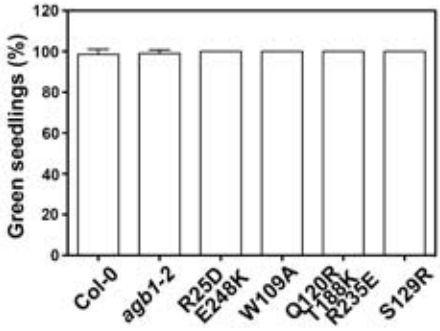

Figure S2. Osmotic control for the glucose-sensing assay.

WT, *agb1-2*, and transgenic plants were grown a low 2% mannitol (w/v) medium. The percentages of green seedlings were scored after 10 days grown at 23°C. The experiment was repeated three times and data were averaged. The error bars represent SD.

Figure S3

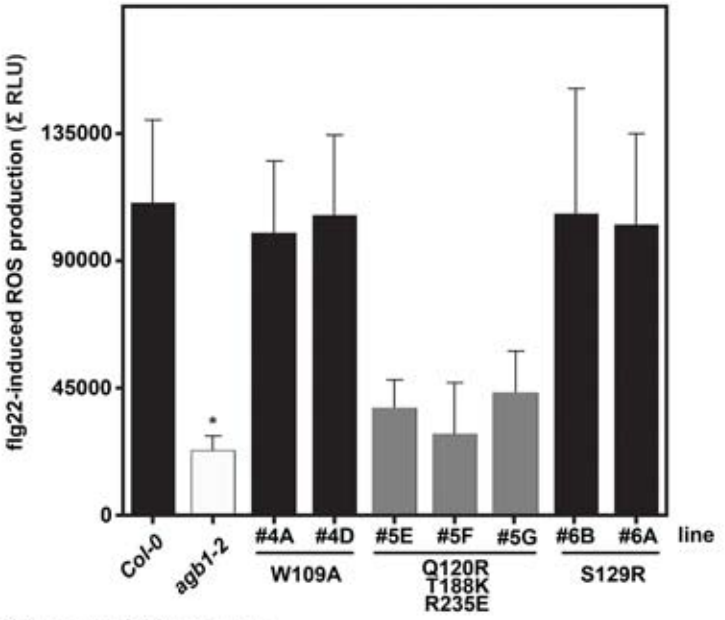

Figure S3. Accumulation of ROS following flg22 treatment.

Leaf discs from 4- to 5-week old plants were treated with 1 µM flg22 and ROS formation was measured as relative light units (RLU) in a chemiluminescence assay during a time course of 38 min after flg22 application. Flg22-induced ROS production in the indicated genotypes (multiple independent lines for each AGB1 variant) is represented as the integrated area under the ROS curve measured and referred to as Σ RLU. The grey scale of bars indicates the extent to which a phenotype was rescued (black = totally rescued, grey = partially rescued, white = not rescued). Data for wild-type plants are plotted in black and those for *agb1-2* mutants are plotted in white. Results are presented as mean ± SE of at least four independent experiments with four to twelve leaf discs per genotype. The asterisk indicates a statistically significant difference (p <0.05; Student's t-test) compared to Col-0.

Figure S4

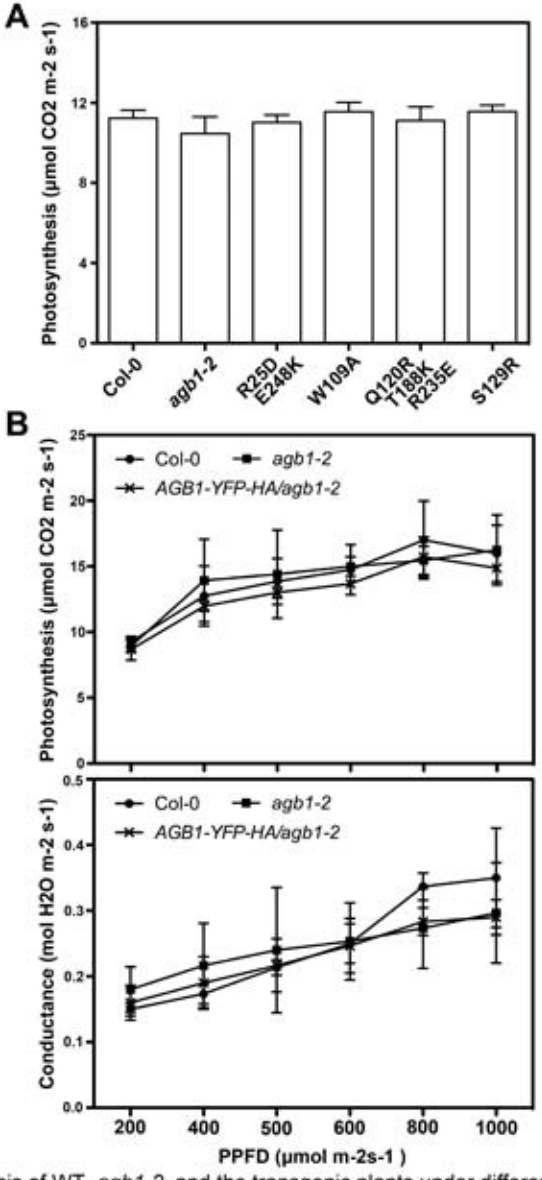

Figure S4. Gas exchange analysis of WT, *agb1-2*, and the transgenic plants under different light intensities.
A, Photosynthesis obtained at PPFD = 500 μmol m^{-2} s^{-1}. Seven plants per genotype were measured in each experiment and data are from one of two independent experiments with same conclusion. No statistically significant difference was found among different genotypes (p >0.05; one-way ANOVA). B, Photosynthesis (upper panel) and stomatal conductance (bottom panel) obtained along a stepwise increase of PPFD. Plants were grown at a constant PPFD (400 μmol $m^{-2}s^{-1}$) before use. Leaves were illuminated with target PPFD values for 5 minutes before each measurement. Three plants per genotype were measured in each experiment. The error bars represent SD. No statistically significant difference was found among different genotypes (p >0.05; two-way ANOVA).

Supplemental Table 1. **Confidence levels for statistical differences in genotype-dependent phenotypes**
Summary of *p*-values from statistical analyses

Phenotype	Non-tagged								10×Myc-tagged							
	R25D E248K		W109A		Q120R T188K R235E		S129R		R25D E248K		W109A		Q120R T188K R235E		S129R	
	WT	*agb1*	WT	*agb1*	WT	*agb1*	WT	*agb1*	WT	*agb1*	WT	*agb1*	WT	*agb1*	WT	*agb1*
Hypocotyl length	<0.001	0.092	0.027	0.002	<0.001	0.103	0.016	<0.001	<0.001	0.784	0.002	0.005	<0.001	0.116	0.002	0.037
Lateral root density	<0.001	<0.001	0.035	<0.001	0.008	0.019	0.845	<0.001	0.005	<0.001	<0.001	<0.001	<0.001	<0.001	0.679	<0.001
Stomatal index	<0.001	0.715	<0.001	0.021	<0.001	0.682	0.754	<0.001	<0.001	0.863	<0.001	0.025	<0.001	0.880	0.542	<0.001
Glucose assay	<0.001	0.632	0.009	0.291	<0.001	0.810	0.007	0.070	<0.001	0.553	0.007	0.224	<0.001	0.523	0.098	0.028
ABA Assay	<0.001	0.681	0.004	0.378	<0.001	0.325	0.276	0.003	0.004	0.427	0.046	0.044	0.013	0.040	0.136	0.014
***F. ox* assay**	<0.001	0.222	0.308	<0.001	<0.001	0.293	0.015	<0.001	<0.001	0.004	0.110	<0.001	<0.001	0.675	0.688	<0.001

Statistical analyses were performed as described in ‘Materials and Methods’. Phenotypic parameters of each transgenic line expressing the indicated variant AGB1 (R25D, E248; W109A; Q120R, T188K, R235E; S129R either tagged or not tagged to Myc) were compared to those of WT and *agb1-2* plants to examine the extent to which a phenotype of *agb1* mutants was rescued. Student *t*-test was adopted for all the phenotypes except ABA responsiveness. The complementation of ABA phenotype was analysed using two-way ANOVA.